



## Translucent zirconia polycrystals prepared from nanometric powders

Radosław Lach\*, Mirosław M. Bućko, Krzysztof Haberko, Marian Rączka, Kamil Wojciechowski

AGH-University of Science and Technology, Al.Mickiewicza 30, 30-059 Kraków, Poland

Received 31 May 2015; Received in revised form 16 August 2015; Received in revised form 25 September 2015; Accepted 29 September 2015

### Abstract

The aim of the present study was investigation of synthesis and sinterability of nanometric zirconia solid solution powders containing 8 mol% and 3 mol% of  $Y_2O_3$ . The powders were prepared by the hydrothermal treatment of the co-precipitated gels, which resulted in very fine powders with particle sizes  $<10$  nm. The main problem in application of such fine powders is their tendency to form hard agglomerates. To overcome this obstacle, the aqueous suspensions of the powders were subjected to the freeze drying. It resulted in the powders composed of very weak agglomerates which were broken under pressure as low as  $\sim 1$  MPa. The powder compacts were sintered in oxygen atmosphere to the state of closed porosity and then HIP-ed at  $1300^\circ\text{C}$  to fully dense ceramics. The spectrophotometric investigations in the wave length range of 190–1100 nm indicated higher translucency of the 8 mol%  $Y_2O_3$ - $ZrO_2$  than the 3 mol%  $Y_2O_3$ - $ZrO_2$  ceramics. Most probably it should be related to the birefringence phenomenon which occurs in the latter case due to the tetragonal symmetry of this material. In the polycrystal containing 8 mol% of  $Y_2O_3$  this phenomenon does not occur due to its cubic symmetry. The other two factors which lead to the decreased optical transparency of the material containing 3 mol%  $Y_2O_3$  are its smaller grain sizes and the presence of some amount of the monoclinic phase.

**Keywords:** nanometric powders, yttria stabilised zirconia, translucence ceramics

### I. Introduction

Solid solutions of yttria in zirconia have been extensively studied due to their unique properties. In the case of the material containing 8 mol%  $Y_2O_3$ , characterized by cubic symmetry [1], its properties as a solid electrolyte have been proved to be useful. Poreless or nearly pore-less polycrystals of this composition have been useful for optical applications, due to their very high refractive index 2.2, which has never been attained in optical glasses. The polycrystals containing 3 mol% of  $Y_2O_3$  show mostly tetragonal symmetry [1]. They are characterized by high fracture toughness. This is related to the martensitic transformation of the tetragonal phase to its monoclinic form at the crack tip running through the material. This transformation consumes elastic energy which otherwise would be used for the crack propagation. That is why such materials show fracture toughness essentially higher than those of zirconia polycrystals of cubic symmetry. However,

the birefringence effects, which occur in the tetragonal polycrystals limit their translucency.

Relatively few investigations have been published on the fabrication methods of theoretically dense zirconia polycrystals containing 8 mol% of  $Y_2O_3$ . In majority of cases the sub-micrometer powders were applied. The effects of some additives (such as titania) to such powders were investigated [2,3]. Different techniques were used for the sintering. Thus, the commercially available sub-micrometer powders were densified by the post-sintering HIP technique [2–5]. Pore closing was performed in vacuum [4–6] or in the oxygen atmosphere. Hot-isostatic pressing led to the pore-free, transparent polycrystals. Spark plasma sintering was also applied in vacuum, using the commercial powder [7] or the powder prepared by the glycine-nitrate process [8]. In the latter case extensive milling of the powder was necessary to remove strong (hard) agglomerates. These agglomerates result from calcination of the powder precursor. During this operation strong contacts between newly crystallized particles develop. Pore size distribution in a powder compact is of utmost importance for

\*Corresponding author: tel: +48126172464, fax: +48126334630, e-mail: radoslaw.lach@agh.edu.pl

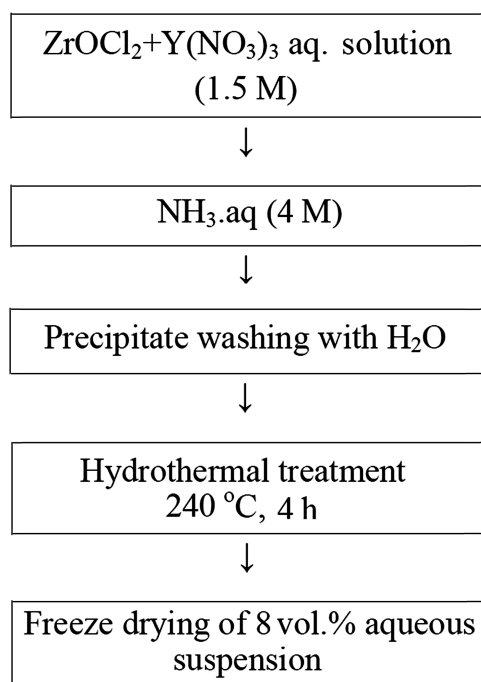


Figure 1. Powder preparation route

the sintering behaviour of the system [9]. Soft agglomerates compacted at sufficiently high pressure lead to the mono-modal and narrow pore size distribution. Dense polycrystals result from sintering of such powders. That is why the agglomerate strength is an important feature of a sinterable powder. According to Rumpf [10] tensile strength of agglomerate is given by the relation:

$$P_c = \frac{9}{8} \cdot \frac{1 - V_p}{\pi d^2} \cdot L_K F_K \quad (1)$$

where:  $V_p$  is pore fraction in an agglomerate,  $L_K$  mean number of contacts per particle,  $F_K$  force necessary to separate two particles in contact and  $d$  particle sizes.

The main problem in application of nanometric powders consists in their tendency to form agglomerates whose strength is controlled by small particle (crystallite) sizes, the force necessary to separate particles and agglomerate porosity.

The aim of the present study was based on the application of the really nanometric zirconia solid solutions powders containing 8 mol% and 3 mol% of yttria. The powders were manufactured by the solid solution crystallization under hydrothermal conditions. The authors' previous studies [11–15] indicated that the process performed in distilled water results in isometric crystallites of nanometric sizes with no first order bonds between particles, i.e. characterized by low  $F_K$  value and hence reducing strength of agglomerates.

## II. Experimental

The preparation method of the powder is described in detail in our previous paper [16]. Figure 1 illustrates the flow sheet diagram of the applied modus operandi.

Both powders, the one of 8 mol%  $Y_2O_3$  (8-YSZ) and the other one of 3 mol%  $Y_2O_3$  (3-YSZ), were prepared by the same method. Table 1 shows the chemical characteristics of the hydrothermally crystallized powders. Hafnium oxide is the main “impurity”. The concentration of yttria with relation to the sum of  $ZrO_2 + HfO_2$  is closed to the assumed values.

Low concentration of the freeze dried suspension of 8-YSZ powder was expected to result in the formation of the agglomerates characterized by high porosity ( $V_p$ ) and hence their low strength. The powder compaction behaviour was studied using Zwick/Roel Z020 machine and the die of 10 mm diameter equipped with the dense zirconia lining. A certain amount of the tested powder was placed in the die. During the processing cycle the ram travel and transmitted load were automatically recorded in the computer memory. Knowing the geometry of the die and the final dimensions of the compact, it was possible to back-calculate the pressure-density response from the load-displacement curve. The applied rate of load increase was 30 N/s up to the final value of 15700 N. This value corresponds to 200 MPa.

For further investigations the samples of 20 mm diameter and 2 mm thickness were uniaxially compacted under 50 MPa and isostatically repressed under 250 MPa. No lubricants were added to the powders. The pressed samples were sintered to the state of closed porosity (1150 °C for 2 h) in oxygen atmosphere and then hot isostatically pressed (HIP) at 1300 °C for 2 h under 250 MPa argon pressure. In our previous work [16] it was found that the oxygen filling closed pores could be easily removed from the system. Since some de-oxidation of the samples occurs during HIP-ing operation, the samples were re-oxidized in air atmosphere at 1000 °C for 1 h and then polished from both sides. Their thickness was 1 mm.

The powder purity was analysed using X-ray fluorescence technique (PANalytical, Axios mAX). The X-ray diffraction (Empyrean, PANalytical) allowed us to determine the powder and the sintered samples phase composition; the powder crystallite sizes on the basis of the X-ray line (111) broadening (Scherrer formula).  $CuK\alpha$  radiation was applied. Powder specific surface area was determined by nitrogen adsorption (Quantochrome Instruments, NOVA 1200e). Pore size distribution in the green samples was measured by mercury porosimetry (PoreMaster 60 Quantochrome Instruments). Density of the HIP-ed samples was determined using helium

Table 1. Chemical characteristics of the powders (impurity concentration in wt.%)

Oxide	Na <sub>2</sub> O	Al <sub>2</sub> O <sub>3</sub>	SiO <sub>2</sub>	NiO	ZrO <sub>2</sub>	Y <sub>2</sub> O <sub>3</sub>	HfO <sub>2</sub>
8-YSZ	0.065	0.023	0.034	0.080	84.227	13.681	1.889
3-YSZ	0.065	0.023	0.034	0.080	92.418	5.318	2.077

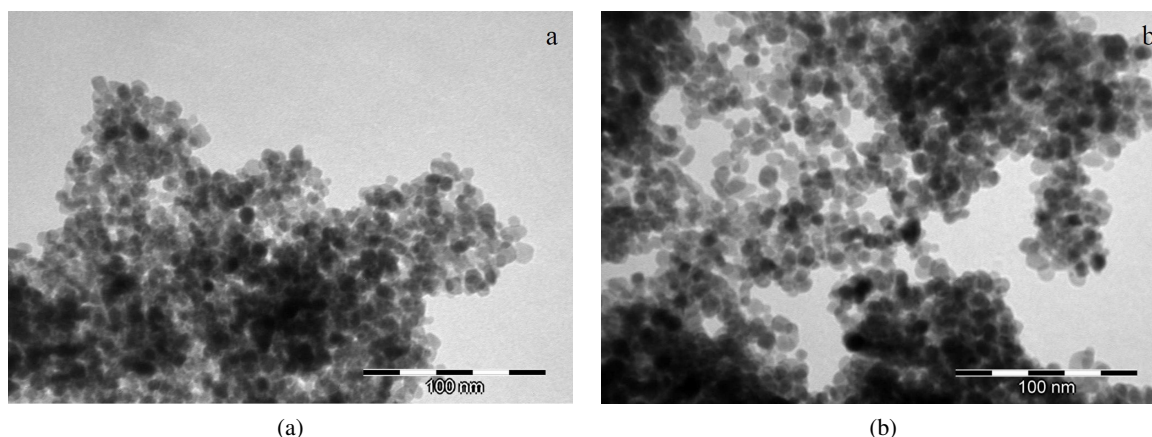


Figure 2. Transmission electron micrographs of the hydrothermally crystallized powders, a) 8-YSZ and b) 3-YSZ

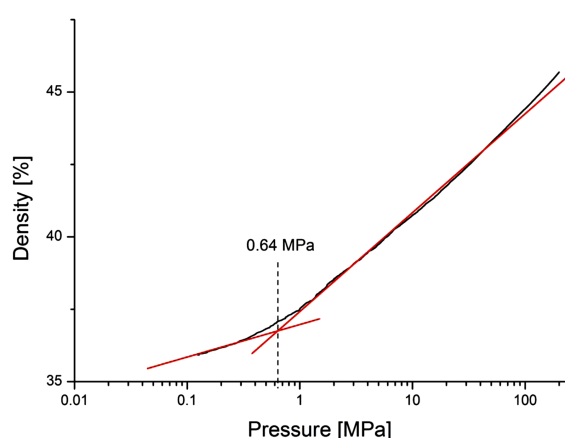


Figure 3. Relative density vs. compaction pressure of the 8-YSZ powder

pycnometer (Micromeritics, AccuPyc II 1340).

The transmission electron microscopy (JEOL-JEM 1011) allowed us to observe powders and assess their crystallite sizes. The mean values of 50 measurements were applied. A scanning electron microscope (Nova Nano SEM 200) was used to characterize microstructure of the dense samples. Their polished surface was thermally etched at 1100 °C for 1 h. The Aphelion (ACIS) computer programme was useful in the quantitative microstructure characteristics. Microstructure of the materials was analysed using the SEM micrographs and the methods described in [17]. On the basis of the equivalent grain diameters observed on the polished surfaces, volume distribution of grains in the three dimensions was found by the Scheil-Schwartz-Sałytkow method. Also 3-dimensional mean grain sizes of both materials were determined.

The optical characteristics were performed using the Jasco V-630 spectrophotometer, operating at the range 190–1100 nm. The V-630 JASCO is a double-beam spectrophotometer with a single monochromator, and a halogen/deuterium lamp is used as a light source. The measurements were provided in the transmittance mode in the wave length range of 350–1100 nm, using an integrating sphere (60 mm diameter) with a scanning speed

of 400 nm/min. For each polished and not-etched sample the measurements were made 3 times and the resulting spectra were the averages of these examinations.

Fracture toughness ( $K_{Ic}$ ) and hardness ( $HV$ ) were measured by the Vickers indentation using the Future Tech (Japan) equipment. Under lower load (1 kg for the sample containing 3 mol% of  $Y_2O_3$  and 0.5 kg in case of the one with 8 mol% of yttria), applied for 15 s to the polished sample surface, no cracks occurred. It allowed us to assess the hardness of the materials. The application of a higher load (3 kg for both materials) led to the Palmqvist cracks. Their length was used to calculate  $K_{Ic}$  according to the formula given in literature [18].

### III. Results and discussion

The average crystallite size ( $D_{111}$ ) and particle size ( $D_{BET}$ ) of each starting powders are close to each other. It indicates that no inter-crystalline boundaries develop during the hydrothermal process. We can also state that crystallites are of isometric shapes, what can be clearly seen in the transmission electron micrographs (Fig. 2).

The load-density response was studied using the powder containing 8 mol% of yttria dissolved in  $ZrO_2$ . The well-established powder characteristics method is based on the observation of its behaviour vs. compaction pressure. In one of the first publications on this problem [19] it was demonstrated that the plot of green density vs. logarithm of compaction pressure the straight line segments would be observed. The fundamental interpretation of this behaviour was suggested by Niesz *et al.* [20]. The point of intersection between the straight line segments corresponds to the pressure under which inter-particle contacts break [9,20]. This method of the powder compaction characteristics was applied mainly in the studies on the sub-micrometric powders compaction behaviour but not in the case of nanometric powders, like those studied in the present work.

Figure 3 illustrates the dependence of density vs. pressure of the 8-YSZ powder which characteristics are shown in Table 2. A similar behaviour is observed in the case of the 3-YSZ powder, not shown here. The point of

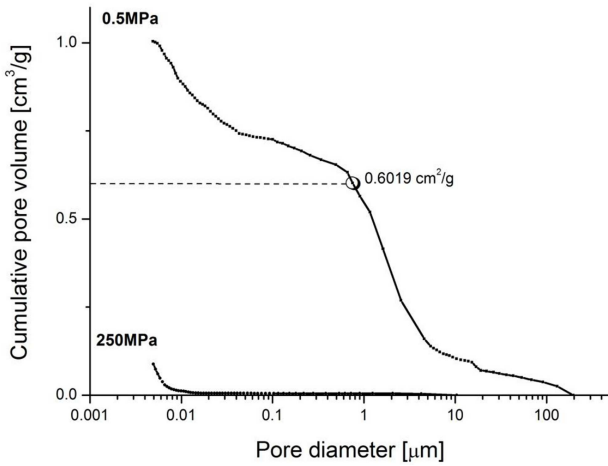


**Figure 4.** Cumulative curve of the pore size distribution in the 8-YSZ powder samples compacted under indicated pressures (arrow indicates volume of pores used in calculation of agglomerate porosity)

**Table 2.** Chemical composition of the glass batches

Feature	8-YSZ	3-YSZ
$D_{111}$ [nm]	8	8
$D_{TEM}$ [nm]	7.9	7.9
$S_w$ [m <sup>2</sup> /g]	126.6	115.7
$D_{BET}$ [nm]	7.9	8.6

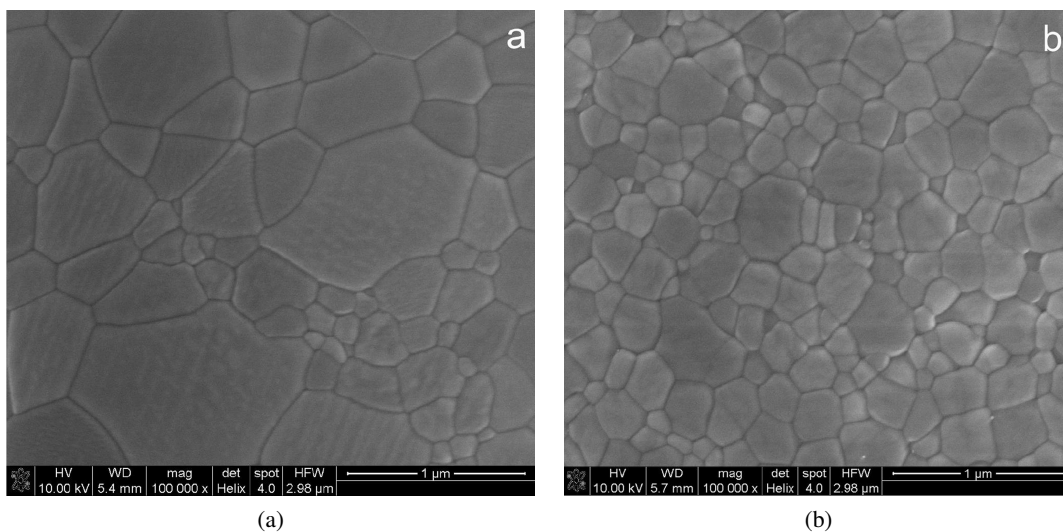
$D_{111}$ : crystallite size calculated on the basis of the X-ray diffraction method from the (111) line broadening,  $D_{TEM}$ : particle sizes observed under transmission electron microscope (mean value),  $S_w$ : specific surface area,  $D_{BET} = 6/\rho S_w$  particle sizes calculated on the basis of the specific surface area,  $\rho$  density of both powders was assumed 6 g/cm<sup>3</sup>

intersection of the two linear sections corresponds to the compaction pressure far below 1 MPa. This is a very low value corresponding rather to the de-cohesion of spray

dried granules [21] than to the behaviour of agglomerates of the nano-powders, prepared by the calcination technique [9]. Pore size distribution measurements (Fig. 4) throw light on the reason of such behaviour of the studied powder. In the case of the compact pressed under 0.5 MPa, i.e. below the point of intersection of the straight line segments, we observe bi-modal pore size distribution (Fig. 4). It indicates the presence of agglomerates in the powder compact. Basing on such a plot, the total porosity can be divided into two parts; the inter-agglomerate and intra-agglomerate pore volume (see a point in Fig. 3). It allows us to assess pore volume within agglomerates (0.6019 cm<sup>3</sup>/g), which can be recalculated to their porosity. It equals as much as 70.7%. This assessment may even be underestimated, since a certain fraction of the smallest pores is beyond the limit of measurements of the applied Hg-porosimeter. To sum up, we can state that such high agglomerate porosity ( $V_p$ ) (and by itself low  $L_K$  value), the lack of strong bonds between crystallites (low  $F_K$ ) (see the formula) explain low pressure under which agglomerates undergo de-cohesion. Therefore, it is quite obvious that no sign of the agglomerate presence occurs in the sample compacted under 250 MPa (Fig. 4).

Scanning electron micrographs of the HIP-ed samples (Fig. 5) indicate that those of the higher yttria concentration are characterized by larger grain sizes. In terms of quantity this difference is illustrated by the data given in Table 3 and cumulative curves of 3-dimensional grain size distribution shown in Fig. 6. The effect of solute concentration on grain sizes in the zirconia systems is known. One of the possible explanations of this phenomenon is suggested by Lange *et al.* [22].

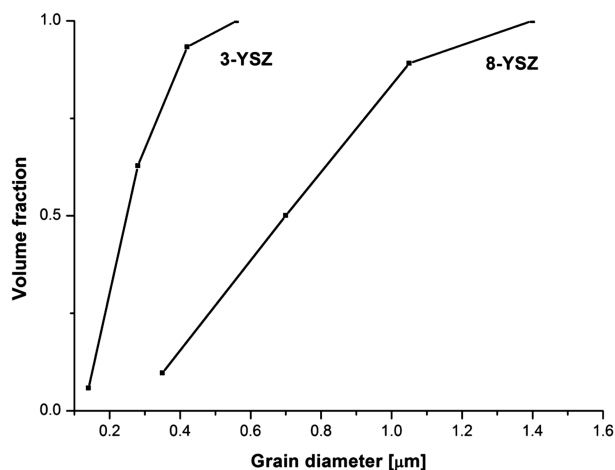
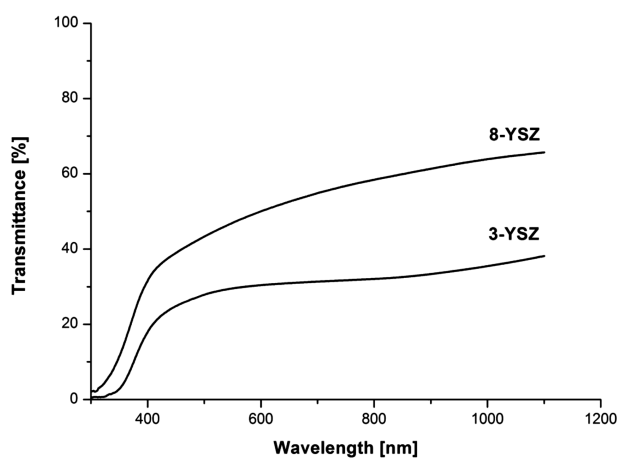
As it should be expected, the ceramics containing 8 mol% of Y<sub>2</sub>O<sub>3</sub> (8-YSZ) shows cubic symmetry and the one with 3 mol% of Y<sub>2</sub>O<sub>3</sub> is mainly tetragonal (92.2%). It contains also 7.8% of the monoclinic phase, most probably formed due to the martensitic transformation of tetragonal phase during surface polishing.



**Figure 5.** Scanning electron micrographs of the ceramics HIP-ed at 1300 °C: a) 8-YSZ, b) 3-YSZ

**Table 3. Properties of the ceramics HIP-ed at 1300 °C**

Ceramics	Grain size [ $\mu\text{m}$ ]	Phase composition	Density [ $\text{g}/\text{cm}^3$ ]	$HV$ [GPa]	$K_{Ic}$ [ $\text{MPa}\cdot\text{m}^{1/2}$ ]
8-YSZ	0.464	cubic	$6.024\pm 0.002$	$9.49\pm 0.39$	$1.75\pm 0.11$
3-YSZ	0.233	92.2% tetragonal 7.2% monoclinic	$6.099\pm 0.001$	$9.41\pm 0.22$	$4.10\pm 0.48$

**Figure 6. Cumulative curves of the 3-dimensional grain size distribution****Figure 7. Translucency of the ceramics HIP-ed at 1300 °C vs. wave length (thickness of the samples equals to 1 mm)**

Density of the samples indicates the total elimination of porosity. That is why light transmittance of the materials is high (Fig. 7), although lower in the case of the system which shows tetragonal symmetry. Optical anisotropy leads to the birefringence effect which limits light transmittance. Essentially smaller grain sizes (Fig. 6) and presence of some monoclinic phase (most probably on the sample surface) should be considered as additional factors limiting light transmittance.

Both materials do not differ from the point of view of their hardness, but show essentially different fracture toughness. The fracture toughness of the material with tetragonal symmetry is much higher. It has been well known for many years that martensitic transformation,

which occurs at the tip of the crack running through the material, is responsible for this effect [23].

#### IV. Conclusions

- It was shown that that nanometric zirconia powders can be used for preparation dense translucent polycrystals.
- Freeze dried hydrothermally crystallized powders consist of agglomerates with extremely high porosity and therefore are mechanically weak.
- Cold compaction of such powders results in the samples which show monomodal pore size distribution.
- The polycrystal containing 8 mol% of  $\text{Y}_2\text{O}_3$  shows cubic symmetry and higher light transmittance than the one with 3 mol% of  $\text{Y}_2\text{O}_3$ . The latter is characterized by the tetragonal symmetry and hence shows birefringence effects which limit light transmittance of the material. Smaller grain sizes and the presence of some monoclinic phase should be considered as additional factors which limit light transmittance of this material.
- Fracture toughness of the tetragonal symmetry material is much higher than shown by the one of cubic symmetry.

**Acknowledgements:** The work was financially supported by the Nacional Science Centre under grant no DEC-2011/03/BST8/06286.

#### References

1. HG. Scott, "Phase relationship in the zirconia-yttria system", *J. Mater. Sci.*, **10** (1975) 1527–1535.
2. K. Tsukuma, "Transparent titania yttria-zirconia ceramics", *J. Mater. Sci. Lett.*, **5** (1986) 1143–1144.
3. K. Tsukuma, I. Yamashita, "Transparent 8 mol%  $\text{Y}_2\text{O}_3$ - $\text{ZrO}_2$  (8Y) ceramics", *J. Am. Ceram. Soc.*, **91** (2008) 813–818.
4. U. Pauchert, Y. Okano, Y. Menke, S. Reichel, A. Ikesuke "Transparent cubic- $\text{ZrO}_2$  ceramics for application as optical lenses", *J. Eur. Ceram. Soc.*, **29** (2009) 283–291.
5. S.R. Casolco, J. Xu, J.E. Garay, "Transparent/translucent polycrystalline nanostructured yttria stabilized zirconia with varying colors", *Scripta Mater.*, **58** (2008) 516–519.
6. J.E. Alniz, F.G. Perez-Gutierrez, G. Aguilar, J.E. Garay, "Optical properties of transparent nanocrystalline stabilized zirconia", *Opt. Mater.*, **32** (2009) 62–68.

7. U. Anselmi-Tamburini, J.N. Woolman, Z. Munir, “Transparent nanometric cubic and tetragonal zirconia obtained by high-pressure pulsed electric current sintering”, *Adv. Funct. Mater.*, **17** (2007) 3267–3273.
8. L. Lei, Z. Fu, H. Wang, S.W. Lee, K. Niihara, “Optical yttria stabilized zirconia from glycine-nitrate process by spark plasma sintering”, *Ceram. Int.*, **38** (2012) 23–28.
9. K. Haberko, “Characteristics and sintering behaviour of zirconia ultrafine powders”, *Ceramurgia Int.*, **5** [4] (1979) 145–148.
10. H. Rumpf, “Grundlagen und Methoden des Granulierens”, *Chemie. Ing. Tech.*, **30** (1958) 144–158.
11. K. Haberko, W. Pyda, “Preparation of Ca-stabilized zirconia micropowders by hydrothermal method”, pp. 774–783 in *Science and Technology of Zirconia II, Advances in Ceramics*, Vol. 12. Eds. N. Claussen, M. Ruhle, A.H. Heuer, The American Ceramic Society, Columbus, OH, 1984.
12. K. Haberko, M.M. Bućko, M. Haberko, M. Jaśkowski, W. Pyda, “Preparation of ceramic micropowders by hydrothermal treatment”, pp. 71–83 in *Freiberger Forschungshefte A779*, VEB Deutscher Verlag für Grundstoff - Industrie, Herstellen und Charakteristiken Feinster Pulver, Teil 2, 1988.
13. W. Pyda, K. Haberko, M.M. Bućko, “Hydrothermal crystallization of zirconia and zirconia solid solutions”, *J. Am. Ceram. Soc.*, **74** (1991) 2622–2629.
14. M.M. Bućko, K. Haberko, M. Faryna, “Crystallisation of zirconia under hydrothermal condition”, *J. Am. Ceram. Soc.*, **78** (1995) 3397–3400.
15. M.M. Bućko, K. Haberko, “Mechanism of the hydrothermal crystallization of zirconia”, pp. 2072 – 2075 in *Euro Ceramics V, Key Engineering* Vol. 132-136, Part 3, Trans Tech Publications, Switzerland, 1997.
16. R. Lach, M.M. Bućko, K. Haberko, M. Sitarz, K. Cholewa-Kowalska, “From nanometric zirconia powder to transparent polycrystal”, *J. Eur. Ceram. Soc.*, **34** (2014) 4321–4326.
17. E.E. Underwood, *Quantitative Stereology*, Addison Wesley Publishing Company, USA, 1970.
18. K. Niihara, P. Morena, P.P.H. Hasselman, “Evaluation of  $K_{Ic}$  brittle solids by indentation method with load-to-indent ratio”, *J. Mater. Sci. Lett.*, **2** (1981) 13–16.
19. C.A. Bruch, “Problems in die pressing submicron size alumina powder”, *Ceram. Age*, **83** (1967) 44.
20. D.E. Niesz, R.B. Bennet, M.J. Snyder, “Strength characterization of powder aggregates”, *Am. Ceram. Soc. Bull.*, **51** (1972) 677–680.
21. G.L. Messing, C.J. Markhoff, L.G. McCoy, “Characterization of ceramic powder compaction”, *Am. Ceram. Soc. Bull.*, **61** (1982) 857–860.
22. F.F. Lange, D.B. Marshall, J.R. Porter, “Controlling microstructures through phase partitioning from metastable precursor: the  $ZrO_2$ - $Y_2O_3$  system”, pp. 519–532 in *Ultrastructure Processing of Advanced Ceramics*. Eds. J.D. MacKenzie, D.R. Ulrich, Wiley and Sons, New York, 1988.
23. R.C. Garvie, R.H.J. Hannink, R.C. Pascoe, “A ceramic steel?”, *Nature*, **258** (1975) 703.